ELSEVIER

Seminars in
NUCLEAR
MEDICINE

Dosimetry of Y-90 Microspheres Utilizing Tc-99m SPECT and Y-90 PET

Bashir A. Tafti, MD, MBA, and Siddharth A. Padia, MD

Dosimetry for yttrium-90 radioembolization continues to generate interest and controversy, as multiple approaches have been used effectively. Traditionally, simple formulas primarily based on patients' body weight or perfused liver volume were used. Over the past several years, dosimetry refinements have led to marked improvements in this therapy from both a safety and efficacy standpoint. Technetium-99m macroaggregated albumin single photon emission computed tomography (SPECT) optimizes pretreatment dosimetry to ensure delivery of a therapeutic radiation dose to the tumor while minimizing nontarget radiation to healthy hepatic tissue. Post-treatment yttrium-90 PET utilizing the inherent internal pair production of yttrium-90 accurately calculates the absorbed dose to tumors and to the normal hepatic parenchyma, which correlates with patient outcomes. As dosimetric calculations become more complex, quantitative imaging with Tc-99m SPECT and Y-90 PET may set the new standard for radioembolization dosimetry.
Semin Nucl Med 49:211-217

Introduction

Yttrium-90 (^{90}Y) radioembolization is now a well-established therapeutic approach to treating nonresectable primary and metastatic liver cancers.[1-4] The normal liver parenchyma receives approximately 80% of its blood supply via the portal vein whereas hepatic malignancies receive 80%-100% of their blood supply from the arterial circulation via hepatic arteries.[1,4] Thus, intra-arterial injection of beta-emitting radionuclides formulated into microspheres preferentially targets the microvasculature of hepatic tumors. The antitumor effects of many radionuclides (eg, phosphorus-32, rhenium-188, and holmium-166 (^{166}Ho)) have been studied.[5] This review will focus on dosimetry of ^{90}Y resin and ^{90}Y glass microspheres using SPECT and PET.

Characteristics

^{90}Y is a beta-emitting radionuclide with average and maximum beta energies of 0.93 and 2.26 MeV, respectively. The average absorbed dose is approximately 50 Gray (Gy) when 1 giga-becquerel (GBq) of ^{90}Y is uniformly distributed across 1 kg of soft tissue.[6] The mean and maximum tissue penetration of the emitted beta particles are 2.5 and 11 mm, respectively.[6,7] ^{90}Y has a physical half-life of 2.67 days (64.2 hours) and thus, about 95% of the radiation dose is delivered within 11 days postadministration. Given its relatively short-half life, limited tissue penetration, and high beta energy, ^{90}Y is an ideal radioembolization agent.[1] Two ^{90}Y formulations are currently approved for clinical use by the United States Food and Drug Administration: resin and glass-based microspheres. SIR-Spheres (SIRTeX Inc) chelate ^{90}Y on the surface of resin microspheres whereas TheraSphere (BTG International Ltd.) incorporate ^{90}Y into glass microspheres. The integration of ^{90}Y into glass microspheres yields a higher specific activity relative to resin microspheres (2500 Bq vs 50 Bq per microsphere), which lowers the number of microspheres required for treatment.[7]

Dosimetry

There is a strong correlation between the radiation dose absorbed by the tumor (ie, target dose) and improvement in progression-free and overall survival.[8-11] On the other hand, excessive radiation to healthy hepatic parenchyma or other organs (ie, nontarget dose) may result in radioembolization-induced liver disease or radiation-induced hepatic fibrosis as

Section of Interventional Radiology, Department of Radiology, David Geffen School of Medicine at University of California Los Angeles, Los Angeles, CA.

Financial Disclosure: SAP is a consultant for BTG International, Bristol Meyer Squibb, and ICON Research. He receives research funding from Boston Scientific Corporation #ISROTH00048.

Address reprint requests to Siddharth A. Padia, MD, Division of Interventional Radiology, Department of Radiology, David Geffen School of Medicine at University of California, Los Angeles, 757 Westwood Plaza, Room 2125, Los Angeles, CA 90095. E-mail: spadia@mednet.ucla.edu

https://doi.org/10.1053/j.semnuclmed.2019.01.005
0001-2998/

well as other radiation-induced complications (eg, gastrointestinal ulceration, radiation pneumonitis, radiation-induced cholecystitis).[12-14] Therefore, accurate prediction of target and nontarget absorbed doses is critical for treatment planning purposes. Empirical dose-response and toxicity studies formed the basis of early dosimetry calculations. Due to the limitations of such primitive methodologies (eg, lack of comparative data, estimating absorbed dose for an "average" individual, etc.), as much as a 10-fold difference is acceptable, radiation dose to the normal liver parenchyma was proposed (ie, 30-390 Gy).[15-17] This likely contributed to suboptimal clinical response and/or significant toxicity observed in early days of radioembolization. Through the use of imaging-guided dosimetry, prediction of a patient-specific absorbed dose has dramatically improved the clinician's ability to maximize therapeutic efficacy and minimize toxicity. The next sections will review current ^{90}Y dosimetry methods, limitations, methodological developments, and future directions in the field.

Pretreatment Dosimetry

At the conclusion of the mapping angiogram, a diagnostic activity of technetium-99m macroaggregated albumin (^{99m}Tc-MAA) is injected into the hepatic artery. This is soon followed by single photon emission computed tomography/computed tomography (SPECT/CT). This serves multiple purposes. The primary purpose is to evaluate and quantify hepatopulmonary vascular shunts.[18-21] This methodology (ie, ^{99m}Tc-MAA scintigraphy) represents a significant improvement in calculation of the lung shunt fraction over planar imaging, which was highly operator-dependent and could overestimate lung shunt fraction by up to 170% compared to SPECT/CT.[21] Based on external-beam radiation therapy data, the highest tolerable pulmonary−absorbed dose has been set at 30 Gy following a single treatment and up to 50 Gy after repeat treatments.[21] The second purpose is to identify potential extrahepatic deposition of radiation into the gastrointestinal tract, which would preclude therapy.[18-21] The final objective of SPECT/CT is optimizing pretreatment dosimetry to ensure delivery of a therapeutic radiation dose to the tumor while minimizing nontarget radiation to healthy hepatic tissue.[9,22-24] This is primarily done by calculating the tumor to nontumor absorbed dose ratio. The most commonly used methods for the latter indication are briefly discussed below.

Activity Planning: Body Surface Area Method (^{90}Y Resin Microspheres)

Based on the assumption that there is a fair correlation between body surface area (BSA) and liver volume in most individuals; BSA, tumor volume, and liver volume are used in this approach to calculate a patient-specific dose of ^{90}Y resin microspheres[2]:

$$\textit{Prescribed activity}\,(GBq) = (BSA - 0.2) + (\textit{Tumor Volume} / \textit{Liver Volume})$$

The calculated dose is reduced when extrahepatic shunting is present (ie, 20% or 40% dose reduction for 10%-15% or 15%-20% shunt fractions, respectively). Treatment is not indicated when the shunt fraction is more than 20%.[2]

This methodology assumes a positive correlation between BSA and total liver volume, which may not hold true for patients with hepatic malignancies. For example, patients with metastatic neuroendocrine tumors will often have a higher liver volume than predicted whereas patients with cirrhosis-associated hepatocellular carcinoma (HCC) may often have smaller liver volumes. This can potentially lead to dose over- or under estimation,[25,26] as demonstrated by Lam et al who reported that BSA-based prescribed doses did not correlate with whole-liver absorbed doses in 45 patients with metastatic colorectal cancer.[26] Furthermore, inaccurate doses may be prescribed for hypo- or hypervascular tumors as the BSA method does not correct for intrahepatic perfusion/distribution differences (commonly calculated by the tumor-to-nontumor ratio).[2]

Activity Planning: Medical Internal Radiation Dose Method (^{90}Y Glass Microspheres)

A simplified version of the Medical Internal Radiation Dose (MIRD) equation determines the time-dependent localization and activity of injected radiation-emitting agents. Presuming: (1) liver to be the only organ absorbing the administered dose and (2) homogeneous intrahepatic distribution of the spheres; this method estimates the mean absorbed dose of ^{90}Y glass microspheres in a targeted area of the liver.[2,27] Hence:

$$\textit{Prescribed activity}\,(GBq) = [\textit{Desired Dose}\,(Gy)\,x\,\textit{Target Volume Mass}\,(Kg)]/50\,(Gy/Kg/GBq)$$

Assuming an average pulmonary mass of 1 Kg, this translates to a maximum of 30 Gy allowable lung dose (or 50 Gy for cumulative treatments), which equals an absolute lung shunt of approximately 600 MBq.[2] Based on this approach, doses ranging from 80 to 150 Gy have been prescribed depending on clinical judgment of the treating physician.[2]

Despite basing the dose on the exact volume of the targeted liver parenchyma, limitations persist. First, the formula assumes an evenly distributed absorbed dose in the perfused tissue. Second, the crossfire phenomenon (ie, tumor irradiation due to microspheres residing in the surrounding healthy liver and vice versa) is not accounted for ref.[22] Dose-point kernel (which factors in the crossfire phenomenon) and Monte-Carlo simulation (which incorporates both tissue heterogeneity and the random nature of particle interactions into model development) methods were subsequently developed to ease some of these concerns. Nevertheless, tedious nature of these methods (taking up to several days) and demanding significant computing resources have hampered their routine and widespread practice.[22]

Activity Planning: Anatomic Partition Model

Initially developed for dosimetry of ^{90}Y resin microspheres and subsequently adopted for dosimetry of ^{90}Y glass microspheres, the anatomic partition model further expanded on the MIRD method by considering the lungs, the tumor, and the healthy liver tissue as separate compartments; and estimating post-treatment activity in each compartment using ^{99m}Tc-MAA SPECT imaging.[10,23,28] The ratio between activity observed in tumor and normal liver compartments ($R_{T/N}$) is calculated as:

$$R_{T/N} = [Tumor\ Activity\ x\ Normal\ Liver\ Mass] / [Normal\ Liver\ Activity\ x\ Tumor\ Mass]$$

wherein activity and mass are expressed in GBq and Kg, respectively. Maximum activity is then calculated as:

$$Prescribed\ activity = D\,x\,\left[\left(R_{T/N}x\,Tumor\ Mass\right) + Normal\ Liver\ Mass\right] / [50\,x\,(1-\mathrm{LSF})]$$

where LSF and *D,* respectively, represent lung shunt fraction and maximum desired absorbed dose by healthy liver in Gy. Activity and mass are again expressed in GBq and Kg.[23,28,29]

The anatomic partition model improves precision dosing because patient-specific anatomical and physiological variables, as well as sequela of prior interventions (eg, surgical resection), are incorporated into the model.[25,28] In support to the latter claim, a good correlation between prescribed activities and tumor-to-normal liver (T/N) ratios or tumor involvement percentage was observed using the partition model, but not the BSA method, suggesting superiority of the partition model in dose planning.[30]

The partition model, however, has remained mostly limited to well-defined tumors because accurate segmentation and quantification of ^{99m}Tc-MAA is a challenging task in disseminated, infiltrative, or poorly delineated malignancies.[2] To overcome this challenge, one institution developed a dual-tracer SPECT fusion imaging protocol.[31] In the latter approach, normal liver parenchyma is delineated by intravenous injection of ^{99m}Tc-Sulfur Colloid and subtracted from the conventional ^{99m}Tc-MAA images to outline areas of tumor involvement.[31]

Absorbed Dose Thresholds

In the early stages of radioembolization therapy development, the actual delivered doses required for effective tumor treatment and avoiding complications were unknown. Earlier retrospective analyses attempting to establish such dose-response relationships suggested an absorbed tumor dose of ≥120 Gy, nontumor whole liver dose of ≤50 Gy, and total lung dose of ≤20 Gy as acceptable levels.[23,32,33] Later studies, however, implied that an antitumor response was not observed up to a tumor absorbed dose of 150 Gy[11] while absorbed doses of ≥205 Gy were predictive of tumor response, disease-free survival, and overall survival in patients with HCC.[34] This was later validated in a larger patient population and in patients with portal vein thrombosis.[10] In addition, toxicity was avoided when the absorbed dose was below 120 Gy (healthy liver) and 30 Gy (lungs).[35] In contrast, the mean TCP_{50} (tumor control probability defined as 50% probability of lesion response) was estimated to be 500 Gy in patients with unilobar HCC, although lesion volume influenced treatment response.[36] For example, TCP_{50} for lesions <10 cm^3 was 250 Gy compared to 1000 Gy for larger lesions. With respect to toxicity, the authors reported a $TD_{15/0.5}$ (defined as tumor dose resulting in 15% risk of severe complications within 6 months) to be 75 Gy for Child-Pugh A patients without complete portal vein obstruction.[36]

^{99m}Tc MAA SPECT/CT Dosimetry Pitfalls

Microsphere distribution maps, as predicted by scout ^{99m}Tc-MAA SPECT/CT, have formed the basis for dosimetry. However, the accuracy and validity of ^{99m}Tc-MAA SPECT/CT predictions have been questioned and the results should be interpreted with caution.

The use of ^{99m}Tc-MAA to plan dosimetry assumes that ^{99m}Tc-MAA and ^{90}Y microspheres follow a similar disposition pattern. However, more recent studies have reported differential distribution patterns.[7,37-45] For instance, a retrospective analysis of 64 ^{90}Y PET/CT scans in patients with advanced HCC reported a weak correlation ($r = 0.27$) between the predicted and actual tumor dose.[42] These observations were in concordance with an earlier study that described >30% difference between the predicted and actual tumor dose in a majority of cases.[45] These discrepancies were also in agreement with dose-response analyses demonstrating a better correlation between tumor absorbed dose and post-treatment dosimetry studies compared to pretreatment dosimetry scans.[5,9]

The underlying reason(s) for the aforementioned mispredictions may be (1) physical differences (eg, differences in the size, number, density, and morphology), (2) technique-related differences (eg, catheter tip position, injections close to bifurcations, injection speed), and (3) physiologic differences (eg, changes in vascular muscle tone and injection time-frame: during blood acceleration, peak or deceleration).[40,43-45] Tumor size and related volume averaging phenomenon can also impact the quantification accuracy of ^{99m}Tc-MAA SPECT/CT and underestimate the calculated absorbed dose. The partial volume effect is more pronounced in lesions ≤3 cm, particularly when tumors are ≤2 cm.[22] Some authors have even cast doubt on the accuracy and reproducibility of ^{99m}Tc-MAA as a biomarker for the lung shunt fraction. For instance, biochemical impurity from circulating free pertechnetate may overestimate the shunt fraction.[46] MAA particles also have highly variable size range (eg, 90% of particles have a long axis between 10 and 90 microns), which can further contribute to different distribution characteristics compared to ^{90}Y microspheres.[2,46] Consequently, patients may receive a suboptimal dose.

There is ongoing research to address these limitations. For example, ^{99m}Tc-labeled albumin spheres (diameter between 10 and 30 microns) have been evaluated.[2] Other investigators are

evaluating resin or albumin microspheres labeled with other positron-emitting isotopes such as fluorine-18 (^{18}F), gallium-68, yttrium-86, and zirconium-89.[47,48] Because such agents are physically similar to therapeutic radioembolization microspheres, their disposition is expected to be similar to ^{90}Y microspheres. This in turn, may improve pretreatment dosimetry. One new agent, ^{166}Ho-loaded poly L-lactic acid microspheres, is commercially available in Europe.[49] An additional advantage of using ^{166}Ho-based agents is that they have paramagnetic properties, allowing them to be visualized by magnetic resonance imaging.[50]

Post-Treatment Dosimetry

Preoperative ^{99m}Tc-MAA dosimetry predicts the distribution of ^{90}Y microspheres. In contrast, post-treatment imaging demonstrates the actual biodistribution of ^{90}Y microspheres[39] and therefore, can help with treatment planning optimization. For example, post-treatment imaging can identify tumors that have received suboptimal radiation exposure, which may indicate a need for repeat super-selective radioembolization or other adjuvant treatment.[51,52] Alternatively, post-treatment imaging may identify high-risk patients for repeat radioembolization if radiation exposure from the initial treatment is considered excessive. Finally, quantitative post-treatment dosimetry data are very important for establishing dose-effect and dose-toxicity correlations. SPECT and PET are the most commonly used imaging modalities for this purpose.

Post-Treatment Dosimetry Using ^{90}Y Scintigraphy

Despite its poor spatial resolution, Bremsstrahlung SPECT is considered standard-of-care for assessing treatment success. Quantifying Bremsstrahlung SPECT photons, however, has proved challenging[43,53,54] due to several factors including wide energy range (0-2.3 MeV), absence of distinct photopeak(s), and faulty image quality caused by penetration of high-energy photons through the collimator septa preventing acquisition of high-resolution images.[53-55] Notwithstanding, elaborate reconstruction algorithms have been developed recently to quantitate ^{90}Y Bremsstrahlung photons with a 5% error margin.[53,56]

In one of the largest clinical studies evaluating ^{90}Y SPECT dose-response dosimetry in patients with HCC ($n = 73$), complete or partial response was observed in 74% of patients with an average absorbed tumor dose of 110 Gy,[33] although others have reported that an absorbed tumor dose of 150-200 Gy may be required.[11,34] One reason underlying these different observations could be the use of various response evaluation criteria (ie, European Association for the Study of the Liver vs Response Evaluation Criteria in Solid Tumors).

Post-Treatment Dosimetry Using ^{90}Y PET/CT Imaging

In comparison to the more commonly used positron-emitting radionuclides such as ^{18}F, ^{90}Y is a poor PET radiotracer as only 32 positrons are emitted per million decays. Thus, PET imaging following ^{90}Y microsphere injection was initially limited as a result of low true-coincidence count rate as well as excessive false-coincidences caused by high-energy Bremsstrahlung X-rays.[43] However, the development of 3D PET/CT scanners equipped with time-of-flight technology has made ^{90}Y PET imaging feasible.[52]

^{90}Y PET/CT has several advantages over pretreatment or post-treatment SPECT-based methods including better spatial resolution and higher precision in quantifying the deposited dose, especially in smaller lesions.[11,53,57-59] The latter characteristics can improve radioembolization treatment planning models by generating more pertinent dose−response and dose-toxicity data. In addition, clinically validated correction and reconstruction techniques developed for other agents (eg, ^{18}F-fludeoxyglucose) can be applied to ^{90}Y PET/CT to generate absorbed dose maps.[52,53,58]

Determining Dose-Response Curves and Increasing Treatment Efficacy Using Quantitative ^{90}Y PET/CT Imaging

Postembolization ^{90}Y PET/CT can expedite assessment of treatment success and subsequent adjuvant therapy (if indicated) by providing highly accurate information regarding ^{90}Y distribution and tumor absorbed dose (Fig.). Several studies have incorporated ^{90}Y PET/CT into treatment-planning algorithms.[51,60] For example, in a patient with tumors involving both lobes of the liver, tumor size in one lobe was used to adjust the injected activity for tumor(s) in the contralateral lobe. The modified dose increased tumor absorbed dose by 40 Gy and led to complete resolution of disease in the treated area within 3 months.[51] In addition, using retrospective analysis of post-treatment ^{90}Y PET data, other authors have shown that a tumor absorbed dose of >200 Gy correlates with better treatment response and prolonged progression-free survival in patients undergoing radioembolization.[11,43,61] The effective absorbed dose threshold also appears to be cancer-type specific, as demonstrated by Kao et al who reported respective D70 (minimum absorbed dose delivered to 70% of tumor volume) thresholds of more than 100 and 90 Gy for complete responders in patients with HCC and cholangiocarcinoma.[62] Variations observed in minimum absorbed dose thresholds are likely due to factors such as small sample size, differences in activity calculation methods, response assessment criteria, microsphere type, and study design.

A recent prospective trial in patients with HCC demonstrated a significantly higher median tumor absorbed dose of 225 Gy compared to 83 Gy in nonresponders. In the latter study, a dose threshold of 200 Gy was 100% specific for objective response and had a 100% positive predictive value whereas all nonresponders received a dose <200 Gy.[63] It should be also noted that as a result of different specific activity, resin and glass ^{90}Y microspheres have disparate dose-response curves. Therefore, clinicians should factor in such differences when applying dose-response data to their clinical practice.

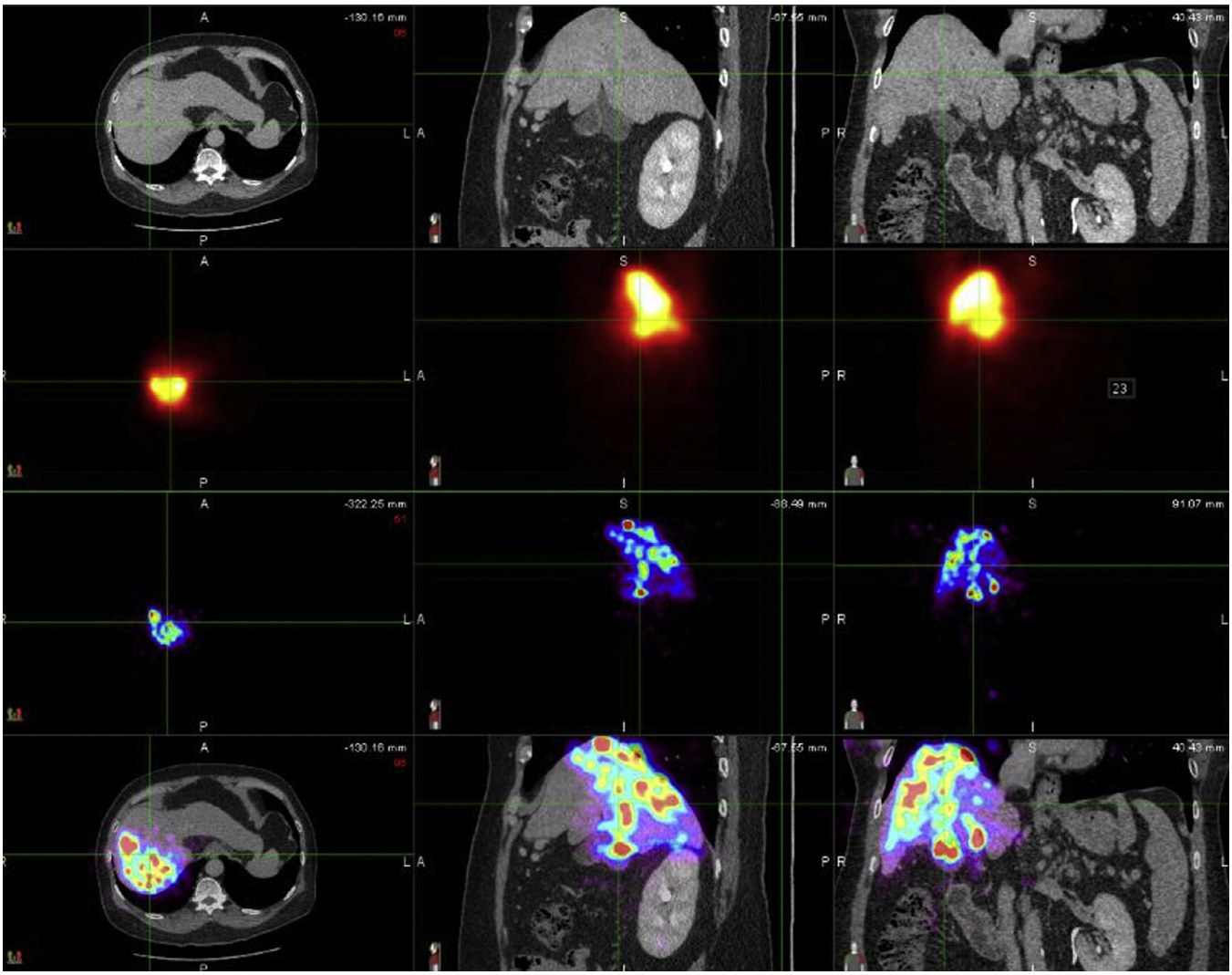

Figure Comparison of Bremsstrahlung SPECT to time of flight PET imaging after radioembolization. After infusion of Y90 microspheres into right hepatic lobe via the right hepatic artery, imaging with Bremsstrahlung SPECT (second row), CT for localization (first row), PET (third row) and PET/CT (fourth row) was obtained. PET images demonstrate a far more detailed map of microsphere deposition showing heterogenous uptake in the right hepatic lobe.

Determining Dose-Toxicity Curves and Improving Treatment Safety Profile Using Quantitative ^{90}Y PET/CT Imaging

Considering the "first, do no harm" notion, establishing the dose-toxicity relationship is perhaps as important as determining the dose-response relationship. Data generated by anatomic partitioning model suggested 70 Gy (50 Gy in cirrhotic patients) as the maximum acceptable nontumor liver absorbed dose for ^{90}Y resin microspheres[2,23] and 120 Gy for glass microspheres.[10] However, the accuracy and reliability of early dose-toxicity recommendations were equivocal because they were mostly based on ^{99m}Tc-MAA pretreatment dosimetry models or retrospective post-treatment Bremsstrahlung SPECT scans which are subject to limitations discussed earlier. For example, such models assumed homogenous distribution of microspheres within the hepatic parenchyma which is most often not true in clinical practice.

To address this knowledge gap, Chan et al conducted a prospective clinical study to determine the acceptable nontumoral liver radiation dose threshold following ^{90}Y radioembolization using PET/CT.[64] The authors reported that the likelihood of developing at least a grade 2 liver toxicity exceeded 50% when the nontumoral liver parenchyma absorbed dose surpassed 54 Gy. The results also indicated that the actual nontumor-delivered dose and Child-Pugh status of the patient are major predicting factors of grade 2 or higher toxicity above the 54 Gy threshold.[64] The findings of the latter investigation were in line with the D_{50} dose-toxicity level of 52 Gy suggested by earlier reports using Bremsstrahlung SPECT imaging.[33,64] Another important implication of the study of Chan et al is that it might be safe for patients who receive minimal nontumor liver dose to undergo repeat radioembolization treatments,[64] although more definitive data are needed to confirm this hypothesis.

Conclusion

Image-guided radioembolization is a rapidly expanding modality for treating primary and metastatic liver cancers. Accurate dosimetry methods enabling physicians to maximize therapeutic efficacy while minimizing toxicity are perhaps the greatest challenge facing the field. Several technical and technological advancements such as enhanced segmentation models and ^{90}Y PET/CT have provided invaluable insight regarding dose-response and dose-toxicity following radioembolization. However, it is now evident that numerous radiobiological and technical parameters (eg, flow dynamics, microsphere specific activity, anatomic variations, tumor type, and disease burden) can affect the outcome and clinicians are now facing more questions than when the field started almost two decades ago. In addition, as innovations in equipment and technique expand the boundaries of radioembolization, new challenges, and safety considerations such as feasibility of repeat radioembolization within the same arterial territory start to emerge. Closing these knowledge gaps warrants further comprehensive prospective clinical studies.

References

1. Ahmadzadehfar H, Biersack HJ, Ezziddin S: Radioembolization of liver tumors with yttrium-90 microspheres. Semin Nucl Med 40:105-121, 2010
2. Braat AJ, Smits ML, Braat MN, et al: 90Y hepatic radioembolization: An update on current practice and recent developments. J Nucl Med 56:1079-1087, 2015
3. Kuei A, Saab S, Cho SK, et al: Effects of yttrium-90 selective internal radiation therapy on non-conventional liver tumors. World J Gastroenterol 21:8271-8283, 2015
4. Rosenbaum CE, Verkooijen HM, Lam MG, et al: Radioembolization for treatment of salvage patients with colorectal cancer liver metastases: A systematic review. J Nucl Med 54:1890-1895, 2013
5. Ahmadzadehfar H, Duan H, Haug AR, et al: The role of SPECT/CT in radioembolization of liver tumours. Eur J Nucl Med Mol Imaging 41 (Suppl 1):S115-S124, 2014
6. Kennedy A, Nag S, Salem R, et al: Recommendations for radioembolization of hepatic malignancies using yttrium-90 microsphere brachytherapy: A consensus panel report from the radioembolization brachytherapy oncology consortium. Int J Radiat Oncol Biol Phys 68:13-23, 2007
7. Tong AK, Kao YH, Too CW, et al: Yttrium-90 hepatic radioembolization: Clinical review and current techniques in interventional radiology and personalized dosimetry. Br J Radiol 89:20150943, 2016
8. Eaton BR, Kim HS, Schreibmann E, et al: Quantitative dosimetry for yttrium-90 radionuclide therapy: Tumor dose predicts fluorodeoxyglucose positron emission tomography response in hepatic metastatic melanoma. J Vasc Interv Radiol 25:288-295, 2014
9. Flamen P, Vanderlinden B, Delatte P, et al: Multimodality imaging can predict the metabolic response of unresectable colorectal liver metastases to radioembolization therapy with Yttrium-90 labeled resin microspheres. Phys Med Biol 53:6591-6603, 2008
10. Garin E, Rolland Y, Edeline J, et al: Personalized dosimetry with intensification using 90Y-loaded glass microsphere radioembolization induces prolonged overall survival in hepatocellular carcinoma patients with portal vein thrombosis. J Nucl Med 56:339-346, 2015
11. Song YS, Paeng JC, Kim HC, et al: PET/CT-based dosimetry in 90Y-microsphere selective internal radiation therapy: Single cohort comparison with pretreatment planning on (99m)Tc-MAA imaging and correlation with treatment efficacy. Med 94:e945, 2015
12. Gil-Alzugaray B, Chopitea A, Inarrairaegui M, et al: Prognostic factors and prevention of radioembolization-induced liver disease. Hepatology 57:1078-1087, 2013
13. Riaz A, Lewandowski RJ, Kulik LM, et al: Complications following radioembolization with yttrium-90 microspheres: A comprehensive literature review. J Vasc Interv Radiol 20:1121-1130, 2009
14. Sangro B, Martinez-Urbistondo D, Bester L, et al: Prevention and treatment of complications of selective internal radiation therapy: Expert guidance and systematic review. Hepatology 66:969-982, 2017
15. Gabrielson A, Miller A, Banovac F, et al: Outcomes and predictors of toxicity after selective internal radiation therapy using yttrium-90 resin microspheres for unresectable hepatocellular carcinoma. Front Oncol 5:292, 2015
16. Lam MG, Abdelmaksoud MH, Chang DT, et al: Safety of 90Y radioembolization in patients who have undergone previous external beam radiation therapy. Int J Radiat Oncol Biol Phys 87:323-329, 2013
17. Son SH, Jang HS, Jo IY, et al: Significance of an increase in the Child-Pugh score after radiotherapy in patients with unresectable hepatocellular carcinoma. Radiat Oncol 9:101, 2014
18. Hamami ME, Poeppel TD, Muller S, et al: SPECT/CT with 99mTc-MAA in radioembolization with 90Y microspheres in patients with hepatocellular cancer. J Nucl Med 50:688-692, 2009
19. Lenoir L, Edeline J, Rolland Y, et al: Usefulness and pitfalls of MAA SPECT/CT in identifying digestive extrahepatic uptake when planning liver radioembolization. Eur J Nucl Med Mol Imaging 39:872-880, 2012
20. Salem R, Parikh P, Atassi B, et al: Incidence of radiation pneumonitis after hepatic intra-arterial radiotherapy with yttrium-90 microspheres assuming uniform lung distribution. Am J Clin Oncol 31:431-438, 2008
21. Yu N, Srinivas SM, Difilippo FP, et al: Lung dose calculation with SPECT/CT for 90-yittrium radioembolization of liver cancer. Int J Radiat Oncol Biol Phys 85:834-839, 2013
22. Garin E, Rolland Y, Laffont S, et al: Clinical impact of (99m)Tc-MAA SPECT/CT-based dosimetry in the radioembolization of liver malignancies with (90)Y-loaded microspheres. Eur J Nucl Med Mol Imaging 43:559-575, 2016
23. Lau WY, Kennedy AS, Kim YH, et al: Patient selection and activity planning guide for selective internal radiotherapy with yttrium-90 resin microspheres. Int J Radiat Oncol Biol Phys 82:401-407, 2012
24. Sangro B, Gil-Alzugaray B, Rodriguez J, et al: Liver disease induced by radioembolization of liver tumors: Description and possible risk factors. Cancer 112:1538-1546, 2008
25. Kao YH, Tan EH, Ng CE, et al: Clinical implications of the body surface area method versus partition model dosimetry for yttrium-90 radioembolization using resin microspheres: A technical review. Ann Nucl Med 25:455-461, 2011
26. Lam MG, Louie JD, Abdelmaksoud MH, et al: Limitations of body surface area-based activity calculation for radioembolization of hepatic metastases in colorectal cancer. J Vasc Interv Radiol 25:1085-1093, 2014
27. Gulec SA, Mesoloras G, Stabin M: Dosimetric techniques in 90Y-microsphere therapy of liver cancer: The MIRD equations for dose calculations. J Nucl Med 47:1209-1211, 2006
28. Ho S, Lau WY, Leung TW, et al: Partition model for estimating radiation doses from yttrium-90 microspheres in treating hepatic tumours. Eur J Nucl Med 23:947-952, 1996
29. Kao YH, Hock Tan AE, Burgmans MC, et al: Image-guided personalized predictive dosimetry by artery-specific SPECT/CT partition modeling for safe and effective 90Y radioembolization. J Nucl Med 53:559-566, 2012
30. Bernardini M, Smadja C, Faraggi M, et al: Liver selective internal radiation therapy with (90)Y resin microspheres: Comparison between pretreatment activity calculation methods. Phys Med 30:752-764, 2014
31. Lam MG, Goris ML, Iagaru AH, et al: Prognostic utility of 90Y radioembolization dosimetry based on fusion 99mTc-macroaggregated albumin-99mTc-sulfur colloid SPECT. J Nucl Med 54:2055-2061, 2013
32. Kokabi N, Galt JR, Xing M, et al: A simple method for estimating dose delivered to hepatocellular carcinoma after yttrium-90 glass-based radioembolization therapy: Preliminary results of a proof of concept study. J Vasc Interv Radiol 25:277-287, 2014
33. Strigari L, Sciuto R, Rea S, et al: Efficacy and toxicity related to treatment of hepatocellular carcinoma with 90Y-SIR spheres: Radiobiologic considerations. J Nucl Med 51:1377-1385, 2010
34. Garin E, Lenoir L, Rolland Y, et al: Dosimetry based on 99mTc-macroaggregated albumin SPECT/CT accurately predicts tumor

response and survival in hepatocellular carcinoma patients treated with 90Y-loaded glass microspheres: Preliminary results. J Nucl Med 53:255-263, 2012
35. Garin E, Lenoir L, Edeline J, et al: Boosted selective internal radiation therapy with 90Y-loaded glass microspheres (B-SIRT) for hepatocellular carcinoma patients: A new personalized promising concept. Eur J Nucl Med Mol Imaging 40:1057-1068, 2013
36. Chiesa C, Mira M, Maccauro M, et al: Radioembolization of hepatocarcinoma with (90)Y glass microspheres: Development of an individualized treatment planning strategy based on dosimetry and radiobiology. Eur J Nucl Med Mol Imaging 42:1718-1738, 2015
37. Chiesa C, Maccauro M, Romito R, et al: Need, feasibility and convenience of dosimetric treatment planning in liver selective internal radiation therapy with (90)Y microspheres: The experience of the National Tumor Institute of Milan. Q J Nucl Med Mol Imaging 55:168-197, 2011
38. Chiesa C, Mira M, Maccauro M, et al: A dosimetric treatment planning strategy in radioembolization of hepatocarcinoma with 90Y glass microspheres. Q J Nucl Med Mol Imaging 56:503-508, 2012
39. Haste P, Tann M, Persohn S, et al: Correlation of technetium-99m macroaggregated albumin and yttrium-90 glass microsphere biodistribution in hepatocellular carcinoma: A retrospective review of pretreatment single photon emission CT and post−treatment positron emission tomography/CT. J Vasc Interv Radiol 28:722-730, 2017
40. Jiang M, Nowakowski FS, Wang J, et al: Characterization of extrahepatic distribution of Tc-99m macroaggregated albumin in hepatic perfusion imaging studies prior to yttrium-90 microsphere therapy. Cancer Biother Radiopharm 26:511-518, 2011
41. Kao YH, Tan EH, Teo TK, et al: Imaging discordance between hepatic angiography versus Tc-99m-MAA SPECT/CT: A case series, technical discussion and clinical implications. Ann Nucl Med 25:669-676, 2011
42. Lea WB, Tapp KN, Tann M, et al: Microsphere localization and dose quantification using positron emission tomography/CT following hepatic intraarterial radioembolization with yttrium-90 in patients with advanced hepatocellular carcinoma. J Vasc Interv Radiol 25:1595-1603, 2014
43. Pasciak AS, Bourgeois AC, McKinney JM, et al: Radioembolization and the dynamic role of (90)Y PET/CT. Front Oncol 4:38, 2014
44. Van de Wiele C, Maes A, Brugman E, et al: SIRT of liver metastases: Physiological and pathophysiological considerations. Eur J Nucl Med Mol Imaging 39:1646-1655, 2012
45. Wondergem M, Smits ML, Elschot M, et al: 99mTc-macroaggregated albumin poorly predicts the intrahepatic distribution of 90Y resin microspheres in hepatic radioembolization. J Nucl Med 54:1294-1301, 2013
46. Lambert B, Mertens J, Sturm EJ, et al: 99mTc-labelled macroaggregated albumin (MAA) scintigraphy for planning treatment with 90Y microspheres. Eur J Nucl Med Mol Imaging 37:2328-2333, 2010
47. Schiller E, Bergmann R, Pietzsch J, et al: Yttrium-86-labelled human serum albumin microspheres: Relation of surface structure with in vivo stability. Nucl Med Biol 35:227-232, 2008
48. Selwyn RG, Avila-Rodriguez MA, Converse AK, et al: 18F-labeled resin microspheres as surrogates for 90Y resin microspheres used in the treatment of hepatic tumors: A radiolabeling and PET validation study. Phys Med Biol 52:7397-7408, 2007
49. Smits ML, Nijsen JF, van den Bosch MA, et al: Holmium-166 radioembolisation in patients with unresectable, chemorefractory liver metastases (HEPAR trial): A phase 1, dose-escalation study. Lancet Oncol 13:1025-1034, 2012
50. van de Maat GH, Seevinck PR, Elschot M, et al: MRI-based biodistribution assessment of holmium-166 poly(L-lactic acid) microspheres after radioembolisation. Eur Radiol 23:827-835, 2013
51. Chang TT, Bourgeois AC, Balius AM, et al: Treatment modification of yttrium-90 radioembolization based on quantitative positron emission tomography/CT imaging. J Vasc Interv Radiol 24:333-337, 2013
52. Lhommel R, van Elmbt L, Goffette P, et al: Feasibility of 90Y TOF PET-based dosimetry in liver metastasis therapy using SIR-Spheres. Eur J Nucl Med Mol Imaging 37:1654-1662, 2010
53. Elschot M, Vermolen BJ, Lam MG, et al: Quantitative comparison of PET and Bremsstrahlung SPECT for imaging the in vivo yttrium-90 microsphere distribution after liver radioembolization. PLoS One 8:e55742, 2013
54. Roshan HR, Azarm A, Mahmoudian B, et al: Advances in SPECT for optimizing the liver tumors radioembolization using yttrium-90 microspheres. World J Nucl Med 14:75-80, 2015
55. Elschot M, Nijsen JF, Dam AJ, et al: Quantitative evaluation of scintillation camera imaging characteristics of isotopes used in liver radioembolization. PLoS One 6:e26174, 2011
56. Rong X, Du Y, Ljungberg M, et al: Development and evaluation of an improved quantitative (90)Y Bremsstrahlung SPECT method. Med Phys 39:2346-2358, 2012
57. Kao YH, Steinberg JD, Tay YS, et al: Post-radioembolization yttrium-90 PET/CT - part 1: Diagnostic reporting. EJNMMI Res 3:56, 2013
58. Kao YH, Tan EH, Ng CE, et al: Yttrium-90 time-of-flight PET/CT is superior to Bremsstrahlung SPECT/CT for postradioembolization imaging of microsphere biodistribution. Clin Nucl Med 36:e186-e187, 2011
59. Padia SA, Alessio A, Kwan SW, et al: Comparison of positron emission tomography and Bremsstrahlung imaging to detect particle distribution in patients undergoing yttrium-90 radioembolization for large hepatocellular carcinomas or associated portal vein thrombosis. J Vasc Interv Radiol 24:1147-1153, 2013
60. Bourgeois AC, Chang TT, Bradley YC, et al: Intraprocedural yttrium-90 positron emission tomography/CT for treatment optimization of yttrium-90 radioembolization. J Vasc Interv Radiol 25:271-275, 2014
61. Srinivas SM, Natarajan N, Kuroiwa J, et al: Determination of radiation absorbed dose to primary liver tumors and normal liver tissue using post-radioembolization (90)Y PET. Front Oncol 4:255, 2014
62. Kao YH, Steinberg JD, Tay YS, et al: Post-radioembolization yttrium-90 PET/CT - part 2: Dose-response and tumor predictive dosimetry for resin microspheres. EJNMMI Res 3:57, 2013
63. Chan KT, Alessio AM, Johnson GE, et al: prospective trial using internal pair-production positron emission tomography to establish the yttrium-90 radioembolization dose required for response of hepatocellular carcinoma. Int J Radiat Oncol Biol Phys 101:358-365, 2018
64. Chan KT, Alessio AM, Johnson GE, et al: Hepatotoxic dose thresholds by positron-emission tomography after yttrium-90 radioembolization of liver tumors: A prospective single-arm observational study. Cardiovasc Intervent Radiol 41:1363-1372, 2018